



Field study on the behavior of pre-bored grouted planted pile with enlarged grout base

Jia-jin Zhou^{1,2} · Jian-lin Yu¹ · Xiao-nan Gong¹ · M. Hesham El Naggar³ · Ri-hong Zhang⁴

Received: 3 July 2020 / Accepted: 2 April 2021 / Published online: 29 June 2021
© The Author(s), under exclusive licence to Springer-Verlag GmbH Germany, part of Springer Nature 2021

Abstract

This paper presents the results of field tests performed to investigate the compressive bearing capacity of pre-bored grouted planted (PGP) pile with enlarged grout base focusing on its base bearing capacity. The bi-directional O-cell load test was conducted to evaluate the behavior of full scale PGP piles. The test results show that the pile head displacements needed to fully mobilize the shaft resistance were 5.9% and 6.4% D (D is pile diameter), respectively, of two test piles, owing to the large elastic shortening of pile shaft. Furthermore, the results demonstrated that the PHC nodular pile base and grout body at the enlarged base could act as a unit in the loading process, and the enlarged grout base could effectively promote the base bearing capacity of PGP pile through increasing the base area. The normalized base resistances (unit base resistance/average cone base resistance) of two test piles were 0.17 and 0.19, respectively, when the base displacement reached 5% D_b (D_b is pile base diameter). The permeation of grout into the silty sand layer under pile base increased the elastic modulus of silty sand, which could help to decrease pile head displacement under working load.

Keywords Base bearing capacity · Enlarged grout base · Grout · PHC nodular pile · Pre-bored grouted planted pile

1 Introduction

Pile foundations are extensively used in high-rise buildings, high speed railway projects, offshore platforms and wind turbines to provide vertical and lateral bearing capacity. The driven pre-stressed high strength concrete (PHC) pile and auger cast-in-situ pile (drilled shaft) are widely used deep foundations [8, 10]. Driven PHC piles are usually used because of their large mobilized shaft and base resistances, while the auger cast-in-situ piles are widely used because the pile diameter and length can be adjusted easily according to the geological conditions.

Nevertheless, both driven PHC and auger cast-in-situ piles have some disadvantages. Driven PHC pile installation process causes noise and vibration, which is harmful to the surrounding facilities [15], and the bearing capacity of auger cast-in-situ pile is often hampered by the mudcake layer at the pile–soil interface and the remaining soil cuttings under pile base [2]. The uncertainty of pile shaft quality (the structural integrity of the shaft) is also a main concern for the auger cast-in-situ pile. Moreover, the auger cast-in-situ pile will produce large amounts of slurry, which can pose a pollution concern to the environment.

The bored precast pile is an innovative piling system that is introduced by some Japanese researchers [4, 16]. In the bored precast pile installation process, a piling rig is employed to drill the pile hole, and grout is injected into the pile hole simultaneously to be mixed with the soil in the hole. A precast (PHC) pile is then inserted into the created hole that is filled with grout body. The bearing capacity of bored precast pile has been demonstrated to be better than the bearing capacity of conventional auger cast-in-place pile [4]. Furthermore, because the precast pile forms the core of the pile, it eliminates any concern related to the quality of pile shaft. Recently, a new jetted and grouted

✉ Jian-lin Yu
yujianlin72@126.com

¹ Research Center of Coastal and Urban Geotechnical Engineering, Zhejiang University, Hangzhou, China

² Institute of Industrial Science, University of Tokyo, Meguro, Tokyo, Japan

³ Department of Civil and Environmental Engineering, Western University, London, Canada

⁴ Faculty of Architectural, Civil Engineering and Environment, Ningbo University, Ningbo, China

precast pile is introduced in North America [12]. The jetted and grouted precast pile also uses a precast pile as the core pile. The jetting of the precast pile can minimize the noise and vibration in the pile installation process and the grouting along the shaft and at the base can increase the shaft and base resistance.

The pre-bored grouted planted (PGP) pile is a new composite pile foundation recently developed in China. The PGP pile is similar to the bored precast pile and the jetted and grouted precast pile. The installation process of PGP pile has been described in detail elsewhere [18], and it can be summarized in four steps: (1) Excavate the pile hole employing a suitable piling rig; (2) Construct an enlarged grout base by expanding the auger to the design base diameter when the auger reaches the target depth of pile base, and inject grout into the enlarged base; (3) Inject grout along the pile hole, mix the grout with soil in the pile hole while moving the auger upward and downward; and (4) Insert the PHC pile into the pile hole under its own weight (i.e., by gravity) to form the complete PGP pile. The PHC nodular pile is commonly adopted as the core PHC pile to increase the frictional capacity of PHC pile–grout interface. The PHC nodular pile has been introduced in detail elsewhere [21], and the 600 mm (800 mm at nodules) PHC nodular pile and 500 mm (650 mm at nodules) PHC nodular pile are often used in practical projects. For the 600 mm PHC nodular pile, the diameter of pile shaft is 600 mm, and the diameter of nodule is 800 mm. The nodules are distributed every certain distance along the pile shaft, and the distance of neighboring nodules is 1000 mm. The PGP pile installation process introduces little disturbance to the surrounding soil, and the use of PHC pile ensures the shaft quality. Moreover, the grout body along the PHC pile shaft and at the enlarged base can improve the shaft and base capacity of PGP pile. Zhou et al. [19, 20] evaluated the bearing capacity of PGP piles from small scale model tests and field load tests and demonstrated that the PGP pile offered higher load carrying capacity than comparable auger cast-in-situ pile.

The enlarged grout body base of PGP pile is similar to the post-grouted body at auger cast-in-situ pile base. Post-grouting under pile base has been proved to be an effective approach to improve the base bearing capacity of cast-in-situ piles [7, 13, 14]. The pile base resistance is a significant component of the capacity for piles with enlarged base; however, it is difficult to measure the base resistance and displacement, especially for long piles. Usually, the base resistance is approximated by the measured axial force of the pile shaft close to the pile base, and the base displacement is estimated by subtracting the elastic shortening of pile shaft from pile head displacement. The base bearing capacity of the enlarged grout base of the PGP pile is still not well characterized due to lack of field test data.

Therefore, this paper investigates the base bearing capacity of PGP pile through bi-directional O-cell load tests on full scale PGP piles.

2 Ground conditions

The field tests described in this paper were performed in Southeast China. The test site comprised deep muddy clay and silty clay layers with high water content and low strength. A series of in-situ tests including cone penetration tests (CPTs) and standard penetration tests (SPTs) were performed, and conventional laboratory tests were also conducted on soil samples retrieved from different elevations. The test site consisted of (starting from top): a 3-m-thick fill layer; a 2-m-thick muddy clay layer; a 1.5-m-thick clayey silt layer; and a 11-m-thick muddy clay layer with high water content (48.7%, larger than liquid limit 43.3%) and low strength. The muddy clay layer overlay two silty clay layers, approximately 20-m-thick. The silty clay layer overlay a 4.5-m-thick sandy silt layer, a 12-m-thick silty sand layer and a 5-m-thick silty clay layer. The soil profiles and soil properties determined from the soil investigation are presented in Fig. 1, in which E_s is the compressive modulus of soil layer and the value of E_s corresponded to the effective pressure in the range 100–200 kPa. The ground water table was about 1.0 m below the ground surface.

The profiles of cone tip resistance (q_c) for CPT sounding and blow count (N) for SPT conducted in the vicinity of the test piles are depicted in Fig. 2. It is noted from Fig. 2 that variation trend of CPT results corresponded with the SPT results. The cone tip resistance of the top 20 m was very small and was almost constant with depth. The blow count of the top 20 m was also very small, and the value of blow count was in the range 1.0–2.0, except in the thin clayey silt layer. The cone tip resistance then increased almost linearly from 20 to 38 m, and the blow count also increased steadily from 2 to 5.5 in the two silty clay layers. The average cone tip resistance in the sand silt layer was about 3.2 MPa, and the average blow count was 14.6 in this layer. The cone tip resistance reached a maximum value in the silty sand layer, and the average value of cone tip resistance was about 18 MPa. The average blow count also reached the maximum value 60.1 in the silty sand layer. The silty sand layer was chosen as the bearing stratum, and all test pile bases were embedded in this layer.

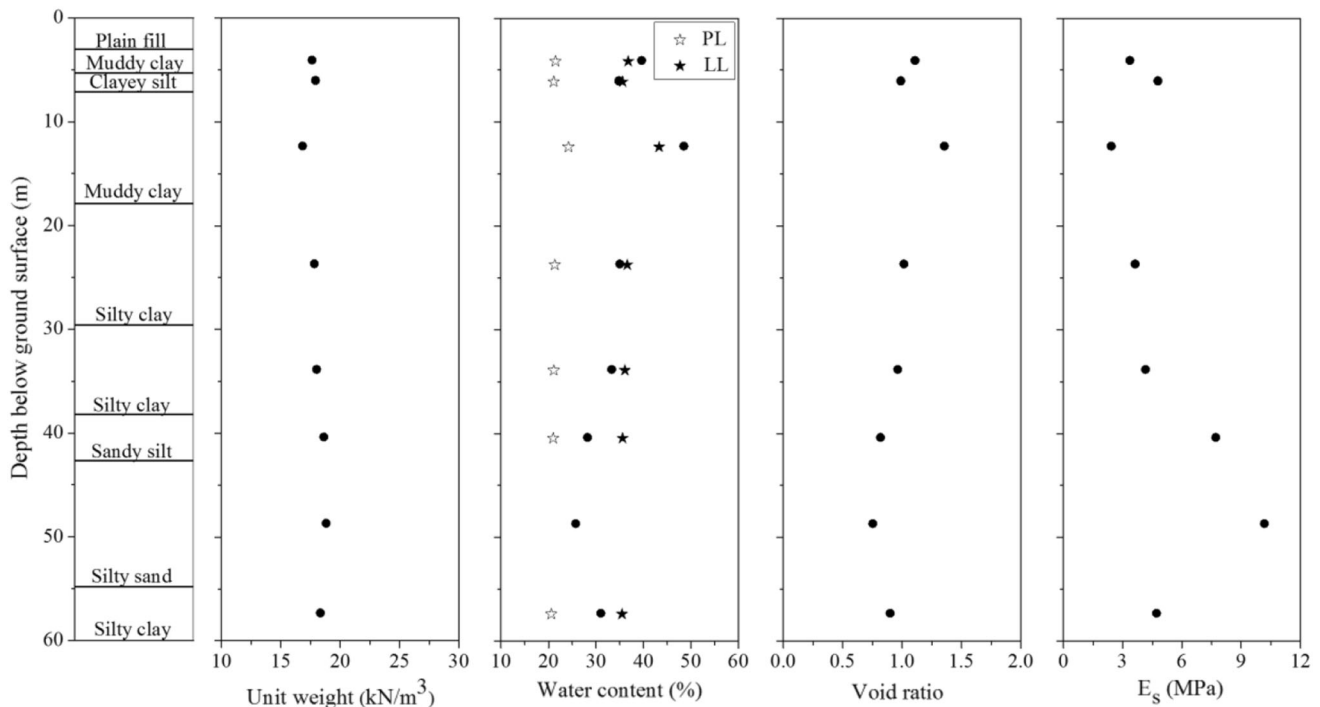


Fig. 1 Soil profiles and properties

3 Test pile details

Two test piles, TP1 and TP2 were installed to investigate the compressive bearing capacity of PGP pile with enlarged grout base. Figure 3 presents the schematic diagram of the test piles. The pile diameter was 750 mm, and its length was 46 m. The upper 31.0 m of each PGP pile was composed of a 600 mm PHC pipe pile, and the lower part of the pile was composed of 500 mm PHC nodular pile (650 mm at nodules) inserted into the grout column of a diameter of 750 mm as shown schematically in Fig. 3. The different segments of PHC piles were welded together before being inserted into the pile hole. The axial load transferred through the pile shaft decreased because of the mobilized shaft resistance, and thus the structural capacity of the pile shaft at the lower part need not to be as high as the upper part. Hence, the diameter of PHC pile at the lower part was 500 mm while the diameter of the upper part was 600 mm. The wall thickness of 600 mm PHC pipe pile and 500 mm PHC nodular pile were 130 mm and 125 mm, and the corresponding cross-section areas were 0.192m^2 and 0.147m^2 , respectively. The ultimate compressive strength of concrete of PHC pile shaft was 80 MPa after being cured for 28 days. The structural compressive capacity of 600 mm PHC pipe pile shaft and 500 mm PHC nodular pile shaft were 15,360 kN and 11,760 kN, respectively. Moreover, a nodule existed every 1 m along the shaft of the lower part to increase its frictional capacity

at the pile–grout interface. Figure 3 also shows that the test PGP pile had an enlarged grout base, and the diameter and height of the enlarged grout base were 1125 mm and 2250 mm, respectively.

The bi-directional O-cell test method was adopted to evaluate the compressive bearing capacity of test piles. As shown in Fig. 3, the O-cell was welded between the two PHC nodular pile segments, and the length of two PHC nodular piles was 12 m and 3 m, respectively. The position of O-cell was 3 m above pile base. Moreover, vibrating wire strain gauges were attached to the steel reinforcement cage of PHC nodular pile in groups of three at 1 m above the O-cell. The range of strain gauge was 0–200 MPa, the sensitivity was 0.12% F·S, and the working temperature was -20 to $+80$ °C. In the strain gauge installation process, the cables of strain gauges were also attached to the rebars of the steel reinforcement cage. Moreover, the length of cables should be long enough to reach the ground surface for the measurement of strain gauge data. The cables which need to thread the upper PHC piles should be fixed at one end of steel reinforcement cage steadily, to protect the cables in the PHC pile manufacture process. The function of the strain gauges was to check the load applied on the upper pile shaft by the O-cell. The test pile shaft was not equipped with strain gauges at other places, as this research was mainly to investigate the base bearing capacity of PGP pile. The location of balance point of pile shaft was very important in bi-directional O-cell test. The

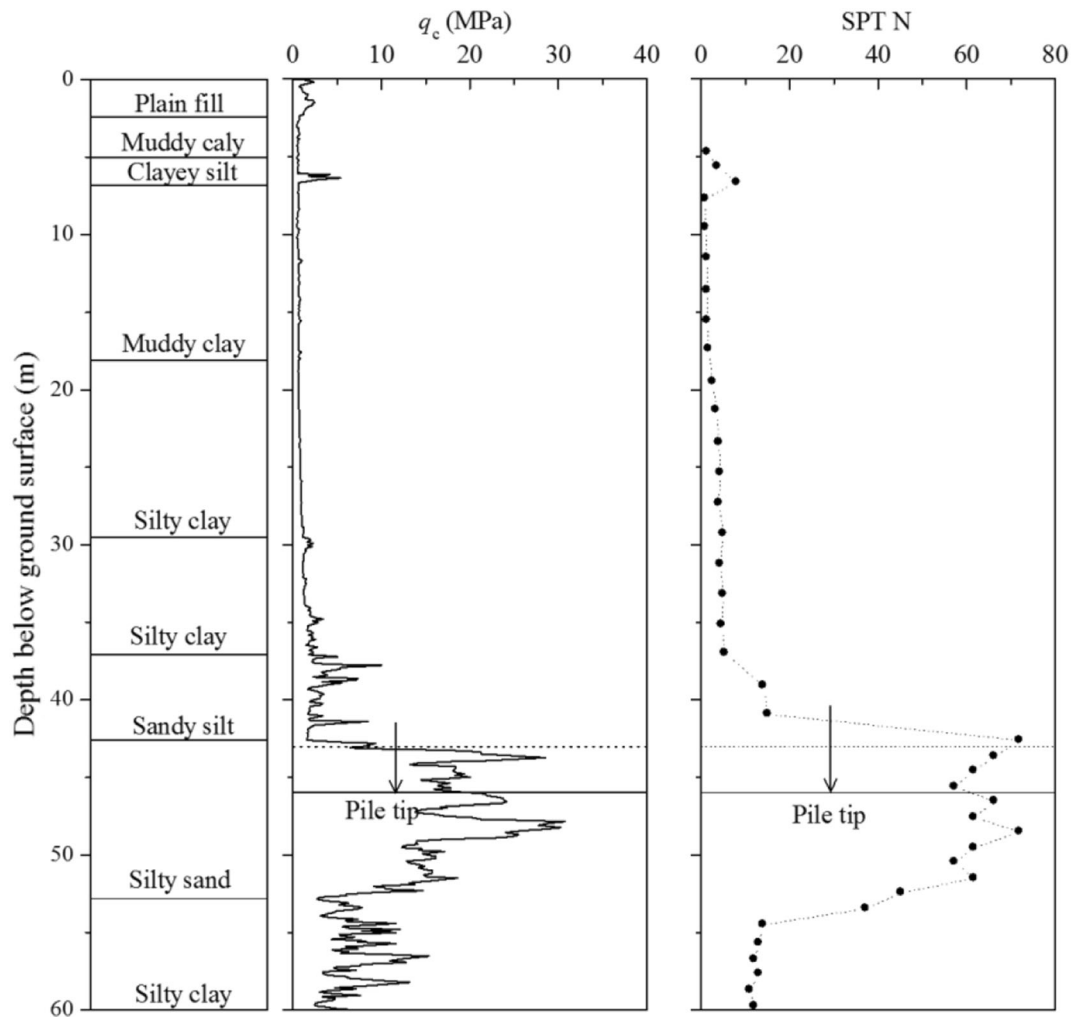


Fig. 2 Cone penetration test and standard penetration test results

PGP pile was a new type of pile foundation, and the shaft and base bearing capacity of PGP pile was still not well understood. According to the soil profiles and properties presented in Figs. 1 and 2, the shaft resistance of pile shaft above the O-cell was about 3050 kN, based on the recommended skin frictions for cast-in-situ piles under compression. Moreover, an uplift coefficient or conversion coefficient should be adopted in calculating the shaft resistance of pile shaft above the O-cell owing to the different loading directions, and the value of conversion coefficient was in the range 0.8–1.0 in clay soil layers [11]. The shaft resistance of pile shaft above the O-cell was in the range 2440–3050 kN. The shaft resistance of pile shaft under the O-cell was 370 kN, and the calculated base resistance of enlarged grout body base was about 2480 kN based on the recommended unit base resistance for non-displacement pile. The sum of shaft and base resistance under the O-cell was 2850 kN. It can be considered that the O-cell was placed around the balance point of pile shaft.

Figure 4 presents photographs of the test pile installation process. Figure 4a shows the piling rig used for the installation of test piles. In the pile hole excavation process, the penetration rate was about 4 m/min in the muddy clay layers, 3 m/min in the silty clay layers, 2 m/min in the sandy silt layer and 1 m/min in the silty sand layer. The rotation speed of the auger was 20 r/min. The diameter of the auger could be expanded when it reached the designed pile base depth to construct the enlarged grout body base. The drilling pipe of the piling rig was also used as the grouting conduit, and the pile hole would be filled with grout after the drilling and grouting process was completed. The model test and simulation results showed that the grout body along the shaft acted as a transition layer and the stress in the grout body along the shaft was very small, while the enlarged grout body base should account for part of base resistance. The strength of grout body at the enlarged base should be large enough to avoid internal failure between enlarged grout body and PHC pile base

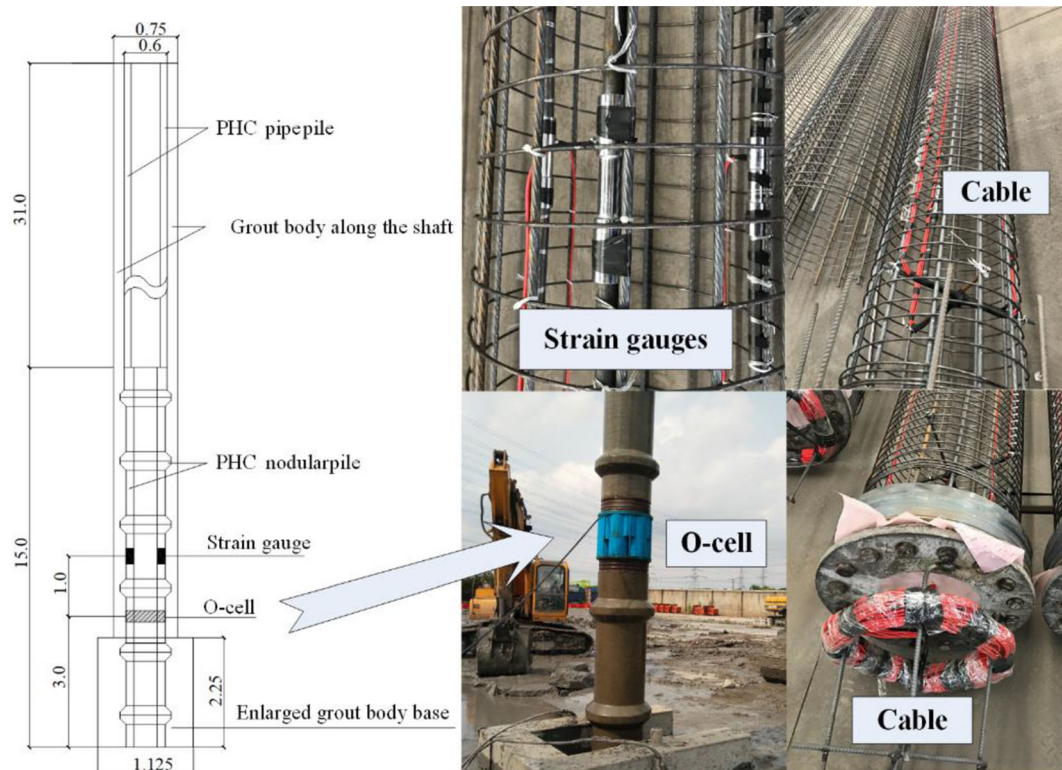


Fig. 3 Schematic diagram of test pile (unit: m)

[17]. In the enlarged grout base construction process, the grout with a water–cement ratio of 0.6 was injected into the enlarged base, and the volume of injected grout should be equal to the calculated volume of the enlarged base. The grouting pressure was about 1 MPa, and the flow rate of the grout was 200 L/min.

The water–cement ratio of the grout injected along the pile shaft was 1.0, and the volume of injected grout was half the volume of pile hole. According to the laboratory test results, the unconfined compressive strength of pure grout with a 1.0 water–cement ratio was about 15 MPa after being cured for 28 days. The grout was mixed with the soil in the pile hole in grout column construction process, and the mass ratio of the grout sample was $m_{\text{cement}}: m_{\text{water}}: m_{\text{soil}} = 1.0: 3.7: 5.3$. The auger should make a sufficient upward and downward motion to guarantee that the grout body along the shaft was homogeneous. The resistance on the auger could be measured by the monitor system of the piling rig, and the grout body along the pile shaft could be considered to be homogeneous when the resistance on the auger became constant in the drilling process.

Figure 4b shows the PHC pipe pile and PHC nodular pile being inserted into the grout column under their own weight. The different segments of PHC pipe pile and PHC nodular pile were welded together before installation, and the strain gauges cables were threaded through the hollow

core of PHC pile. The speed of pile insertion process was about 20 m/min, as the pile hole was filled with homogeneous grout body, and the resistance in PHC pile insertion process was very small.

4 Static load tests

According to the local technical specification for pile testing [1], the grout body in PGP pile should be allowed to cure for at least 28 days before the static load test is conducted. The test piles TP1 and TP2 were cured for 52 days and 55 days, respectively, before the bi-directional O-cell load test were conducted. The schematic of bi-directional O-cell load test is presented in Fig. 5. It can be seen from Fig. 5 that the O-cell applied the load on both the upper and lower pile segments during the loading process, and the loads applied on both directions were always the same. The counter force for the base resistance of enlarged grout base was provided by the self-weight and shaft resistance of the upper pile segment. Furthermore, four steel pipes were placed within the hollow core of PHC pipe pile and PHC nodular pile, and a displacement string was placed in each steel pipe. The steel pipes were welded at the inner surface of PHC pipe pile and PHC nodular pile before the PHC pile being inserted into the pile hole. Two displacement strings were used to measure the displacement of enlarged grout



Fig. 4 PGP pile installation process

base, and the other two displacement strings were used to measure the displacement of the pile segment above the O-cell.

According to the local specification [11], the value of load increment should be 1/10 of the maximum applied load, and the value of first load increment should be twice the value of other load increments. In this research, the bearing capacity of enlarged grout body base was not well understood, and the value of load increment was set to be 1/20 of the estimated maximum base resistance to gain the full load–displacement curves of the test piles. The first load increment in the bi-directional O-cell load test was 300 kN, and the subsequent increments were 150 kN each. The settlements were also measured after each load increment at an interval of 5 min, 15 min, 30 min, 45 min, 60 min, 90 min, 120 min until the settlement is less than 0.1 mm within every 1 h.

5 Test Results

The bi-directional O-cell load test results can be converted into equivalent pile head load–displacement curves of the conventional static load test. The test results can be converted according to the local specification JGJ/T 403–2017 [11]:

$$Q_u = \frac{Q_1 - W}{\gamma} + Q_2 \quad (1a)$$

$$s = s_2 + \Delta s \quad (1b)$$

$$\Delta s = \frac{[(Q_1 - W)/\gamma + 2Q_2] \cdot L_1}{2E_p \cdot A_p} \quad (1c)$$

in which Q_u and s are the converted pile head load and displacement, respectively; Q_1 and Q_2 are the load applied on the pile segment above and below O-cell, respectively, and $Q_1 = Q_2$; the axial force measured by the strain gauges equipped 1 m above the O-cell was about 150 kN smaller than the value of Q_1 after Q_1 was larger than 600 kN, which indicated that the shaft resistance of pile segment between the O-cell and strain gauges was 150 kN; W is the self weight of pile shaft above the O-cell, the weight of the PHC pile shaft and grout body above the O-cell were 195 kN and 205 kN, respectively, and the total self weight of pile shaft W was 400 kN; s_2 is the measured displacement of the pile segment below O-cell; Δs is elastic shortening of pile shaft; γ is skin friction conversion coefficient, and the recommended value of γ is in the range 0.8–1.0. The value of γ was 0.9 in this research as that the test piles were embedded in clayey soil.

The converted pile head load–displacement responses of the test piles are presented in Fig. 6. This figure shows that the load–displacement responses of two test piles were fairly similar and exhibited three segments: an initial linear segment when the pile head load was less than 3672 kN, followed by a linear segment with a slightly reduced slope when the pile head load increased from 3672 to 5889 kN for TP1 and to 6522 kN for TP2. Finally, the pile head displacement increased sharply when pile head load increased to 6206 kN and 6839 kN, respectively, of TP1 and TP2. Hence, punching failure occurred when the pile head load of TP1 and TP2 increased to 6206 kN and 6839 kN, respectively. According to the local specification [1], the ultimate capacity of TP1 and TP2 were 5889 kN and 6522 kN, respectively. The ultimate compressive capacity of TP2 was about 10% larger than the ultimate compressive capacity of TP1. Considering the variation of soil layer profiles in the test site and the influence of grout body along the pile shaft and at the enlarged base on the behavior of PGP pile, the 10% difference in ultimate compressive capacity of TP1 and TP2 was reasonable.

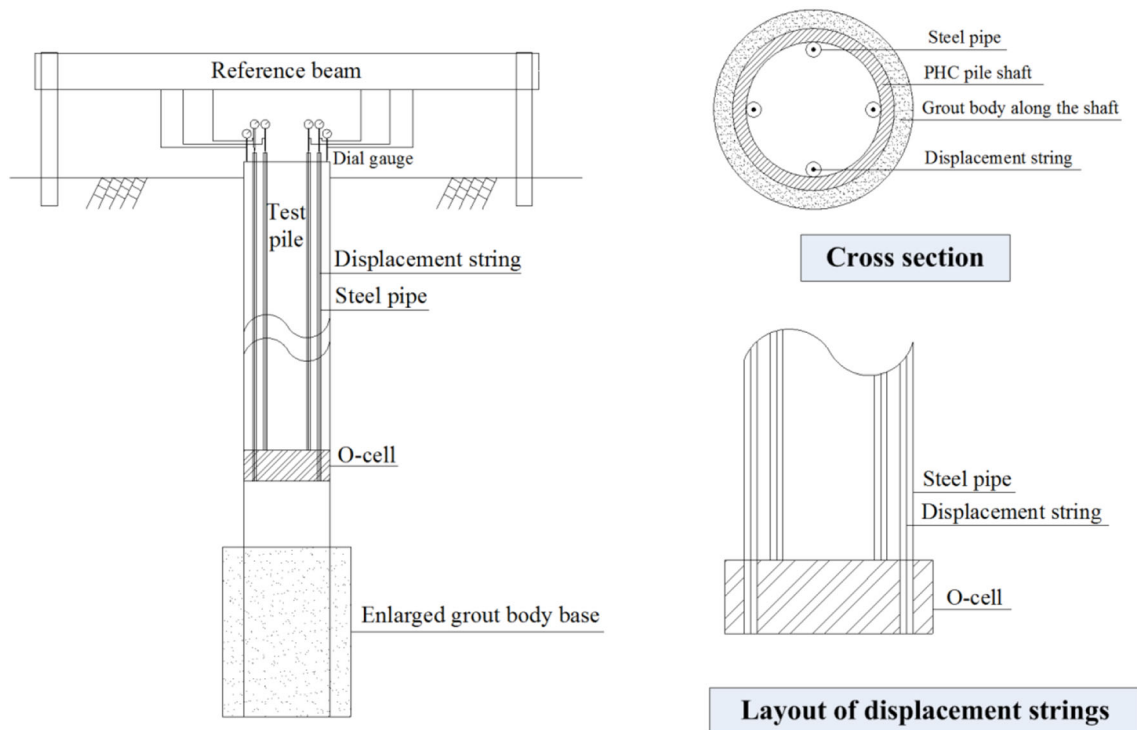


Fig. 5 Schematic of bi-directional O-cell load test

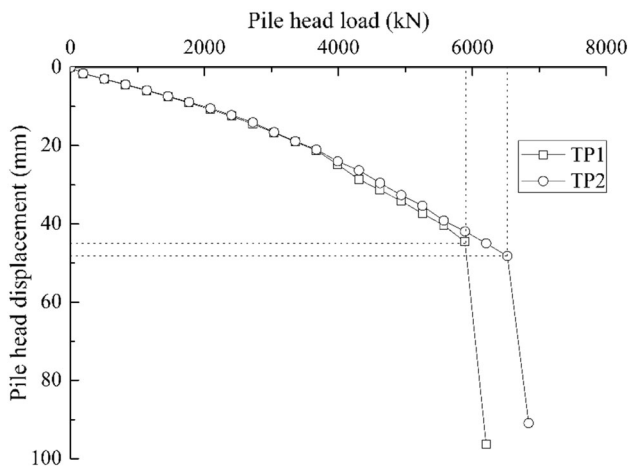


Fig. 6 Load–displacement responses of test piles

The enlarged grout body base was embedded in the silty sand layer, as shown in Fig. 2. The height of the enlarged grout body was 2.25 m, and the O-cell was equipped 3 m above the pile base. Hence, the load applied on the pile segment below O-cell can be approximately taken as the mobilized base load, and the measured displacement of the pile segment below O-cell is taken as the base displacement. The shaft resistance of the test piles can be calculated by subtracting the pile head load with the corresponding base resistance. The average skin friction can be calculated by the following equation:

$$\tau_s = Q_s / (\pi \cdot d \cdot L) \tag{2}$$

in which τ_s is average skin friction; Q_s is shaft resistance; d is pile diameter; L is effective pile length.

The PGP pile shaft consisted of a core PHC pipe/nodular pile and the grout body around the PHC pile. Hence, the shaft load transfer of PGP pile occurred through two interfaces: PHC pile–grout interface and grout–soil interface. The test pile could behave as an integral pile only when the failure occurred at the grout–soil interface. The frictional capacity of the PHC pile–grout interface should also be investigated. The clayey soil retrieved from the test site was used to make the grout specimen in the laboratory. The construction of PGP pile involved moving the piling rig upward and downward during the drilling and grouting process, and thus the grout body around the PHC pile was assumed to be homogeneous. The mass ratio of the grout sample made in the laboratory was the same as the mass ratio of the grout body in the field test, i.e., $m_{\text{cement}}: m_{\text{water}}: m_{\text{soil}} = 1.0: 3.7: 5.3$. The grout samples were cast in 70.7 mm × 70.7 mm × 70.7 mm molds to prepare the test specimens for unconfined compressive strength tests, and all the samples were allowed to cure for 52 days in standard curing room. The unconfined compressive strength of the grout samples was 850 kPa. The PHC pile–grout interface shear test was conducted in a specially developed pile–soil interface shear test apparatus which has been described elsewhere [22]. The model PHC pile was

manufactured in advance, and the surface roughness of model PHC pile should be controlled the same as the surface roughness of prototype PHC pile. The homogenous grout sample was then placed around the model PHC pile to prepare the PHC pile–grout interface specimen. The PHC pile–grout interface specimen was then moved into the standard curing room and being allowed to cure for 52 days before the interface shear test. In the PHC pile–grout interface shear tests, the PHC pile–grout interface specimen was under radial confining pressure, and the contact form of the PHC pile–grout interface was identical to that of the prototype pile–soil interface. The displacement of the grout body was constrained by the base plate of the shear test apparatus, to ensure that the failure occurred at the PHC pile–grout interface. The measured ultimate skin friction of the PHC pile–grout interface was 110 kPa, when the strength of grout body was 850 kPa.

Figure 3 shows that the diameter of the PHC pile and the grout body around the PHC pile were 600 mm and 750 mm, respectively. The shaft capacity of PGP pile was controlled by the PHC pile–grout body interface and the grout body–soil interface. The failure of PGP pile shaft would occur at the PHC pile–grout body interface when the shaft resistance of PHC pile–grout body interface was smaller than the shaft resistance of grout body–soil interface, and the PHC pile and grout body could act as an integral pile when the shaft resistance of PHC pile–grout body interface was larger than the shaft resistance of grout body–soil interface.

To guarantee that the PHC pile and grout body act as an integral pile in the load transfer process, the shaft resistance of PHC pile–grout interface should be larger than the shaft resistance of grout–soil interface. The diameter of PHC pile (D_p) was 600 mm, and the diameter of grout body zone (D_c) was 750 mm. The maximum skin friction (f_s) allowed at the grout body–soil interface can be estimated by:

$$f_s = \frac{D_p}{D_c} \cdot f_c \quad (3)$$

in which f_c is the ultimate skin friction of the PHC pile–grout interface, and the value of f_c was 110 kPa according to the PHC pile–grout interface shear test results; the value of D_p/D_c was 0.8 as the value of D_p and D_c was 600 mm and 800 mm, respectively.

Hence, the test piles would act as a unit only when the ultimate skin friction at the grout body–soil interface was less than 88 kPa. Given that the test piles were embedded in mostly clayey soil layers where the ultimate skin friction of grout body–soil interface was less than 88 kPa, TP1 and TP2 would behave as an integral pile with diameter equal to 750 mm.

The variation of the shaft resistance with the pile head displacement of test piles is presented in Fig. 7. It can be seen from Fig. 7 that the average skin friction of TP1 and TP2 were gradually mobilized with the increase of normalized pile head displacement (pile head displacement/pile diameter), and the average skin friction of TP1 and TP2 reached the ultimate value when the normalized pile head displacements increased to 5.9% and 6.4%, respectively. The pile head displacement needed to fully mobilize the shaft resistance was larger than the proposed value (0.5–2% D) by Fleming et al. [2]. This is because that the PHC pipe pile and PHC nodular pile were adopted as the core pile of the test PGP piles, and the wall thickness of 600 mm PHC pipe pile and 500 mm PHC nodular pile were 130 mm and 125 mm, respectively. The cross-section area of 600 mm PHC pipe pile and 500 mm PHC nodular pile were 0.192 m² and 0.127 m², respectively. The Young's modulus of the concrete of PHC pile shaft was 40 GPa. Assume that the axial load of pile shaft decreased linearly from pile head to base, the calculated pile shaft elastic shortening of TP1 and TP2 were 28.6 mm and 31.7 mm, respectively, when the skin friction reached the ultimate value. The value of pile shaft elastic shortening of TP1 and TP2 reached 3.81% D and 4.23% D , respectively, when the shaft resistance was fully mobilized. The pile shaft elastic shortening of PGP pile was larger than the pile shaft elastic shortening of cast-in-situ pile under identical pile head load. Moreover, the ultimate skin frictions of TP1 and TP2 were 28.5 kPa and 31.8 kPa, respectively. The ultimate skin friction of TP1 and TP2 were much smaller than 88 kPa, and the assumption that TP1 and TP2 would behave as an integral pile with diameter equal to 750 mm was reliable.

As mentioned above, the load applied on the pile segment below O-cell can be approximately taken as the

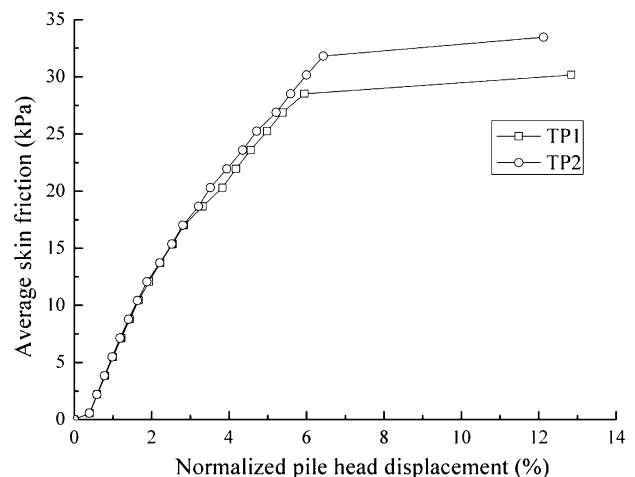


Fig. 7 Variation of average skin friction with normalized pile head displacement

mobilized base load, and the measured displacement of the pile segment below O-cell is taken as the base displacement. The pile base load–displacement curve of TP1 and TP2 are presented in Fig. 8. It can be seen from Fig. 8 that the base load–displacement response of TP1 and TP2 were similar and exhibited three parts: a linear segment when the base resistance was less than 1050 kN, followed by a nonlinear segment when the base resistance was in the range 1050–3000 kN for TP1 and 1050–3300 kN for TP2, and a final linear segment with much reduced slope when the base resistance reached 3150 kN for TP1 and 3450 kN for TP2.

The base resistance is typically fully mobilized at base displacement in the range 5%–10% D_b (D_b is pile base diameter), and even larger for non-displacement piles in granular soil [2]. Figure 8 shows that plunging failure occurred for both TP1 and TP2 in the last loading step, and the base displacement for TP1 and TP2 exceeded 56.25 mm (5% D_b). The pile head displacement also exceeded 10% D in the last loading step. Hence, it can be considered that the ultimate base resistance of TP1 and TP2 were 3120 kN and 3430 kN, respectively, when the base displacement reached 5% D_b .

The height of the enlarged grout base of the test piles was 2250 mm, and its diameter was 1125 mm containing the PHC nodular pile base and the grout base. The test piles were not excavated from the ground after the loading test, and the integrity of the enlarged base was unknown in this research. Nevertheless, Kon et al. [5] excavated the test piles which were also installed by pre-bored piling method after conducting the pile-toe load tests. The unconfined compressive strength of the grout body at the enlarged base was also tested, and the strength of the grout body was in the range 10.9–13.2 MPa. The grout body and nodular pile base were found to be closely bonded with each other after the loading test, and the maximum base resistance was

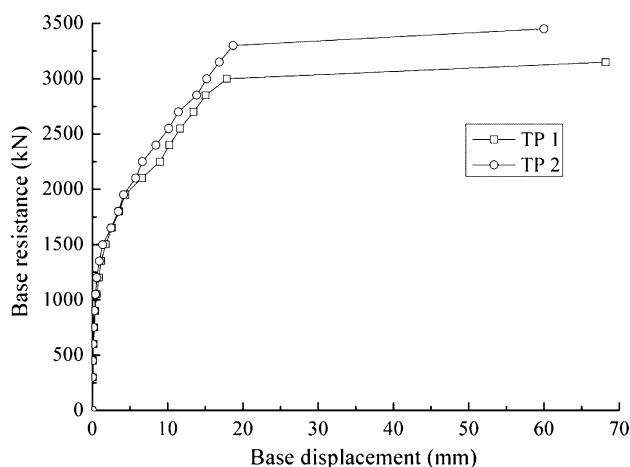


Fig. 8 Base load–displacement response of test piles

5000 kN. The strength of the grout body in this research was 20 MPa, and the maximum base resistances were 3150 kN and 3450 kN, respectively. The shaft resistance of nodular pile base–grout interface in this research was larger than the shaft resistance of nodular pile base–grout interface in Kon’s tests, as the strength of grout at the enlarged base in this research was larger than 13.2 MPa. It can be considered that the PHC nodular pile base and the grout body around the nodular pile base could act as a unit in the loading process, and the base diameter of the test piles was 1125 mm.

The pile base bearing capacity has been extensively investigated by many researchers, and Randolph and Wroth [9] proposed an empirical equation to calculate pile base displacement:

$$s_b = \frac{P_b(1 - \mu)}{4r_b G_b} \quad (4)$$

in which P_b and s_b are the pile base resistance and base displacement, respectively; μ and G_b are the Poisson’s ratio and shear modulus of the soil under pile base, respectively; and r_b is pile base radius.

It can be noted from Fig. 8 that the slope of pile base load–displacement curves reduced with the increase of pile base displacement, owing to the degradation of shear modulus of the soil under pile base. Han and Ye [3] proposed an empirical equation to simulate the degradation of the shearing modulus of the soil under pile base:

$$G_b = G_{b0} \left(1 - R_f \frac{P_b}{Q_b}\right)^2 \quad (5)$$

in which G_{b0} is initial shear modulus of the soil under pile base; Q_b is the ultimate base resistance; and R_f is failure ratio.

The ultimate base resistance of TP1 and TP2 were 3120 kN and 3430 kN, respectively, and the pile base radius was 562.5 mm. Laboratory tests were conducted on the silty sand retrieved from the test site. The Poisson’s ratio of the silty sand was 0.3. The value of elastic modulus of the silty sand changed with vertical effective stress. The value of elastic modulus E_s was 10.2 MPa when the vertical effective stress was in the range 100–200 kPa; E_s value increased to 17.1 MPa when the vertical effective stress was in the range 200–400 kPa; and E_s value finally increased to 29.1 MPa when the vertical effective stress was in the range 400–800 kPa. The vertical effective stress of the silty sand layer in the test site was close to 400 kPa, and the value of E_s was 29.1 MPa. The shear modulus of silty sand can be approximated by,

$$G_b = \frac{E_b}{2(1 + \mu)} \quad (6)$$

The calculated shear modulus of silty sand was 11.2 MPa. Nevertheless, the initial shear modulus of the soil under pile base estimated from the initial section of base resistance–displacement curves of test piles was much larger than 11.2 MPa. The back-calculated initial shear modulus of the soil under pile base from Fig. 8 was about 850 MPa. This is probably because that large amount of grout permeated into the silty sand layer in the enlarged base construction process. The strength of the grout body at the enlarged base was 20 MPa, and its elastic modulus was 2800 MPa. The Poisson's ratio of the grout body was about 0.25, and its shear modulus was 1120 MPa. The property of silty sand under pile base was improved because of the permeation of grout in the enlarged base construction process, and the initial shear modulus of the enhanced silty sand was close to the shear modulus of grout body at the enlarged base. The measured and calculated pile base load–displacement curves are presented in Fig. 9. The dotted curves in Fig. 9 are the calculated base load–displacement curves of TP1, and the solid curves are the calculated base load–displacement curves of TP2. It can be seen from Fig. 9 that the calculated curves can fit well with the measured results when the failure ratio is 0.85. The value of failure ratio is close to 0.9 which is proposed by Han and Ye [3]. Hence, the conventional method can also estimate the base load–displacement response of PGP pile well, when the PHC nodular pile base and grout body at the enlarged base is taken as a unit, and the diameter of grout body zone is taken as the pile base diameter.

The CPT results are also commonly used to estimate the pile base bearing capacity, owing to the similarities between the cone and an axially loaded pile. The PGP pile is a non-displacement pile, and no pressure locked under pile base before the loading test. Fleming et al. [2] proposed a hyperbolic relationship to correlate the unit pile base resistance to the cone tip resistance for non-displacement piles, as follows:

$$\frac{q_b}{q_c} = \frac{s_b/d}{s_b/d + 0.5 \cdot q_c/E_b} \quad (7)$$

in which q_b is unit pile base resistance, s_b is pile base displacement, d is pile base diameter, and E_b is the elastic modulus of the soil under pile base.

The test pile bases were all embedded in the silty sand layer, and the value of cone tip resistance (q_c) of silty sand layer was about 18 MPa according to Fig. 2. The elastic modulus of silty sand under pile base was 29.1 MPa. Nevertheless, it should be noted that the property of silty sand was improved because of the permeation of grout in the enlarged base construction process. The back-calculated initial shear modulus of the silty sand from Fig. 8 was about 850 MPa, which was close to the shear modulus of the grout body at the enlarged base. The elastic modulus of strengthened silty sand can be estimated according to Eq. (6). The Poisson's ratio of strengthened silty sand was assumed to be the same as the Poisson's ratio of grout body. The calculated elastic modulus of strengthened silty sand was 2125 MPa. Moreover, the degradation of elastic modulus of strengthened silty sand in the loading process should also be considered. The base displacement of TP1 and TP2 reached 6.1% and 5.3% D_b , respectively, after the last loading step, and almost plunging failure occurred. Fleming et al. [2] also suggested that the base resistance was typically fully mobilized at base displacement in the range 5%–10% D_b . It can be assumed that the elastic modulus of soil under pile base decreases with the increase of base displacement when base displacement is in the range 0–10% D_b , as follows,

$$E_b = E_{b0} \left(1 - \frac{s_b/D_b}{0.1}\right) \quad (8)$$

in which E_{b0} is initial shear modulus of the soil under pile base.

The variation of normalized base resistance (unit base resistance/average cone tip resistance) with normalized base displacement of test piles is presented in Fig. 10. The dotted line in Fig. 10 represents the normalized base resistance–normalized base displacement response of conventional non-displacement pile (from Eq. 7). It can be seen from Fig. 10 that Eq. (7) can not represent the pile base resistance–displacement response well if the elastic modulus of silty sand (29.1 MPa) is adopted as the elastic modulus of soil under pile base. As expected, the slope of the calculated normalized base resistance–normalized base displacement curve is much smaller than the measured results, as the permeation of grout into the silty sand increased the elastic modulus of silty sand. Hence, the elastic modulus of strengthened silty sand should be adopted in calculating the base load–displacement curve of PGP pile. Moreover, it should be noted that the grout could

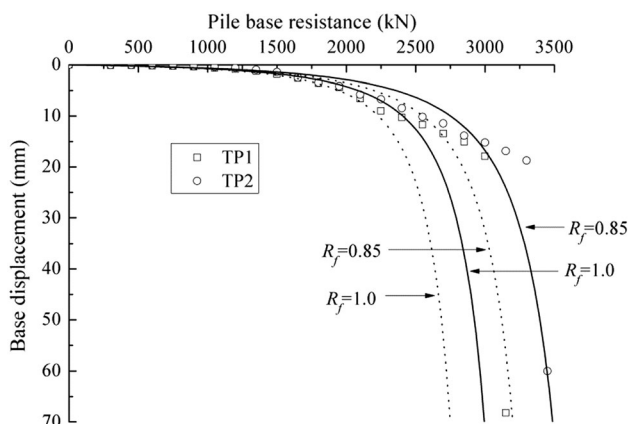


Fig. 9 Calculated and measured pile base load–displacement curves

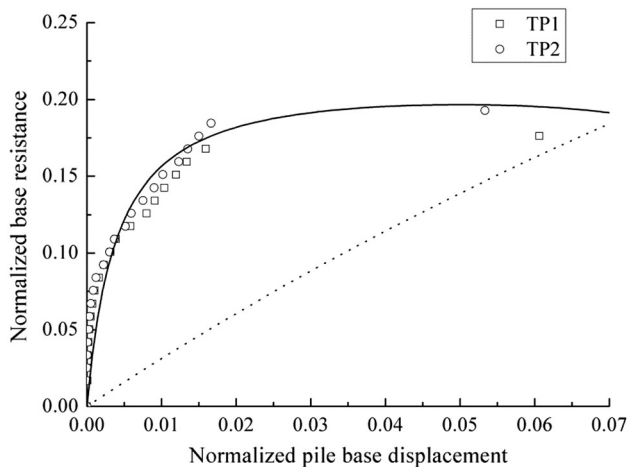


Fig. 10 Variation of normalized base resistance with normalized base displacement

only permeate into the superficial silty sand layer under the pile base, and the pile base load would be transferred to the non-grouted silty sand layer with the increase of base load. The non-grouted silty sand layer was the bearing stratum, and a reduction coefficient R should be adopted for the estimation of base bearing capacity of PGP pile, as follows,

$$\frac{q_b}{q_c} = \frac{R \cdot s_b/d}{s_b/d + 0.5 \cdot q_c/E_b} \quad (9)$$

The solid line in Fig. 10 represents the normalized base resistance–normalized base displacement response by considering the permeation of grout into the silty sand (from Eqs. 8 and 9). Figure 10 shows that Eqs. (8) and (9) can simulate the measured base resistance–displacement response well, when the initial elastic modulus of soil under pile base was 2125 MPa, and the value of reduction coefficient R was 0.23.

Figure 10 also shows that the maximum normalized base resistance was 0.18 for TP1 and 0.19 for TP2. Nevertheless, the design base resistance is normally taken as that mobilized within a limited displacement, rather than a true maximum value. If a base displacement of 5% D_b is taken as the limit base displacement, the normalized base resistance was 0.17 for TP1 and 0.19 for TP2. The value of normalized base resistance for bored pile was found to be in the range 0.1–0.2 [6]. The measured normalized base resistance of test piles were close to the recommended value for bored piles. The permeation of grout into the silty sand under pile base increased the initial elastic modulus of the silty sand, and the initial slope of base resistance–displacement curve of test piles was also much larger than that of conventional bored pile. It should be noted the grout could only permeate into the silty sand layer near the pile base, and eventually the base load would be transferred to the non-grouted silty sand layer. The non-grouted silty sand

layer was the bearing stratum. The ultimate normalized base resistance of test piles were close to the recommended value for bored piles. Nevertheless, it should be noted that the diameter of the enlarged grout base was 2.25 times the diameter of the PHC nodular pile base, and the base area of enlarged grout base was about 5 times the base area of PHC nodular pile. The enlarged grout base effectively increased the pile base resistance through increasing the pile base area. Moreover, a safety coefficient of 2 is often adopted in pile foundation design [2], and the working load is half the value of ultimate load. The base displacement of PGP pile would be much smaller than the base displacement of conventional bored pile under working load, as the initial slope of base load–displacement curve of PGP pile was much larger than that of conventional bored pile.

6 Conclusions

Full-scale pile load tests were conducted to investigate the compressive bearing capacity of PGP pile with enlarged grout base. The bi-directional O-cell test method was conducted on the test piles to give a detailed investigation on the base bearing capacity of PGP pile. Based on the test results presented herein, the following conclusions may be drawn:

1. The load transfer of PGP pile shaft occurred through two interfaces: the PHC pile–grout interface and the grout–soil interface. The skin friction of PHC pile–grout interface was much larger than the skin friction of grout–soil interface for the PGP piles embedded in clayey soil. The pile head displacement needed to fully mobilize the shaft resistance was 5.9% and 6.4%, respectively, of two test piles, because of the large elastic shortening of pile shaft.
2. The PHC nodular pile base and the grout body at the enlarged base could act as a unit in the loading process. The permeation of grout into the silty sand layer under the pile base increased its elastic modulus, and the initial slope of base load–displacement curve of PGP pile was much larger than that of conventional bored pile.
3. The enlarged grout base could effectively promote the base bearing capacity of PGP pile through increasing the base area. The measured normalized base resistance of two test piles were 0.17 and 0.19, respectively, when base displacement reached 5% of pile base diameter. The base displacement of PGP pile under working load was smaller than that of conventional bored pile, which can help to decrease pile head displacement under working load.

Acknowledgements The research described is funded by the Natural Science Foundation of China (Grant No. 51978610). The authors also want to express gratitude to ZCONE High-tech Pile Industry Holdings Co., Ltd. for the financial and technical support with the manufacture and installation of the test PGP piles.

References

- CABR (China Academy of Building Research) (2014) Technical code for testing of building foundation piles. JGJ 106-2014, China Construction Industry Press, Beijing (in Chinese)
- Fleming K, Weltman A, Randolph M, Elson K (2009) Piling engineering, 3rd edn. Taylor & Francis, London
- Han J, Ye SL (2006) A field study on the behavior of micropiles in clay under compression or tension. *Can Geotech Eng* 43(1):19–29
- Horiguchi T, Karkee MB (1995) Load tests on bored PHC nodular piles in different ground conditions and the bearing capacity based on simple soil parameters. *Proc Tech Rep Jpn Archit Soc* 1:89–94
- Kon H, Yshida E, Kabasawa K, Komatsu G, Kuwabara F, Kimura M (2010) Investigation of soil cement around nodular piles after pile-toe load test installed by pre-bored piling method. *Jpn Geotech J* 5(4):615–623 ((in Japanese))
- Lee JH, Salgado R (1999) Determination of pile base resistance in sands. *J Geotech Geoenviron Eng* 125(8):673–683
- Mullins G, Winters D, Dapp, S. (2006) Predicting End Bearing Capacity of Post-Grouted Drilled Shaft in Cohesionless Soils. *J Geotech Geoenviron Eng* 132(4):478–487
- O'Neill MW (2001) Side resistance in piles and drilled shafts. *J Geotech Geoenviron Eng* 127(1):3–16
- Randolph MF, Wroth CP (1978) Analysis of deformation of vertically loaded pile. *J Geotech Eng Div* 104(12):1465–1488
- Randolph MF (2003) Science and empiricism in pile foundation design. *Geotechnique* 53(10):847–875
- The Professional Standards Compilation Group of People's Republic of China (2017) Technical specification for static loading test of self-balanced method of building foundation piles. JGJ/T 403-2017. China Architecture and Building Press, Beijing (in Chinese)
- Thiyyakkandi S, McVay M, Bloomquist D, Lai P (2012) Measured and predicted response of a new jetted and grouted precast pile with membranes in cohesionless soils. *J Geotech Geoenviron Eng* 139(8):1334–1345
- Thiyyakkandi S, Mcvay M, Bloomquist D, Lai P (2014) Experimental study, numerical modeling of and axial prediction approach to base grouted drilled shafts in cohesionless soils. *Acta Geotech* 9(3):439–454
- Wan Z, Dai G, Gong W (2019) Field study on post-grouting effects of cast-in-place bored piles in extra-thick fine sand layers. *Acta Geotech* 14:1357–1377
- White DJ, Finlay TCR, Bolton MD, Bearss G (2002) Press-piling: ground vibration and noise during pile installation. In: *Proceeding of international deep foundations congress*, ASCE, Reston, VA, pp 363–371
- Yamato S, Karkee MB (2004) Reliability based load transfer characteristics of bored precast piles equipped with grouted bulb in the pile toe region. *Soils Found* 44(3):57–68
- Zhou JJ, Gong XN, Wang KH, Zhang RH, Yan TL (2016) A model test on the behavior of a static drill rooted nodular pile under compression. *Mar Georesour Geotechnol* 34(3):293–301
- Zhou JJ, Gong XN, Wang KH, Zhang RH, Yan JJ (2017) Testing and modeling the behavior of pre-bored grouting planted piles under compression and tension. *Acta Geotech* 12:1061–1075
- Zhou JJ, Gong XN, Zhang RH (2019) Model tests comparing the behavior of pre-bored grouted planted piles and a wished-in-place concrete pile in dense sand. *Soils Found* 59(1):84–96
- Zhou JJ, Gong XN, Zhang RH, El Naggar MH, Wang KH (2020) Field behavior of pre-bored grouted planted nodular pile embedded in deep clayey soil. *Acta Geotech* 15:1847–1857
- Zhou JJ, Yu JL, Gong XN, Yan TL (2020) Field tests on behavior of pre-bored grouted planted pile and bored pile embedded in deep soft clay. *Soils Found* 60(2):551–561
- Zhou JJ, Yu JL, Gong XN, El Naggar MH, Zhang RH (2020) The effect of cemented soil strength on the frictional capacity of precast concrete pile–cemented soil interface. *Acta Geotech* 15:3271–3282

Publisher's Note Springer Nature remains neutral with regard to jurisdictional claims in published maps and institutional affiliations.